Reprinted from

Eighth International Symposium

Machine Processing of

Remotely Sensed Data

with special emphasis on

Crop Inventory and Monitoring

July 7-9, 1982

Proceedings

Purdue University
The Laboratory for Applications of Remote Sensing
West Lafayette, Indiana 47907 USA

APPLICATION OF A RECURSIVE DISTORTION ESTIMATOR TO THE GEODETIC CORRECTION OF THEMATIC MAPPER IMAGERY

P. ARNOLD, J. BROOKS, E. KIMMER, I. LEVINE, V. MATTHEWS, D. POROS

General Electric/Space Division
Lanham, Maryland

I ABSTRACT

Landsat-D will have a new higher resolution imaging system in the Thematic Mapper instrument. The higher resolution increases the demands on the accuracy needed by the ground processing in correcting for geodetic errors due to internal misalignments and uncertainties in the knowledge of spacecraft ephemeris and attitude. The Thematic Mapper will also process longer imagery intervals than previous missions. To accomplish the required correction a recursive distortion estimator (Kalman filter) was adapted for use on Thematic Mapper imagery.[1] This method estimates a minimum variance spacecraft state error vector for known initial covariance of the elements of that vector and known image noise.

The recursive distortion estimator was tested with various spacecraft models using a simulation of real world state vector dynamics. The density of control points needed to meet specified geometric correction requirements was determined as a function of imagery interval length and control point measurement error.

II THE LANDSAT-D SYSTEM

The Landsat-D satellite is a continuation of the Landsat series of satellites which for many years have provided useful information for monitoring the earth's resources. The new Landsat, though, presents a significant improvement over previous Landsats. It carries a four-band Multispectral Scanner (MSS) and a Thematic Mapper (TM) imaging instrument designed to provide better spatial and spectral resolution than MSS. The attitude control capability of the Multimission Modular Spacecraft (MMS) has also been improved in both pointing accuracy and stability. In addition, Angular Displacement Sensors (ADS) mounted on the three TM axes will provide information on the "jitter" effects in the imagery.

General Electric is responsible for the Landsat-D spacecraft integration and test (flight segment) and the development of a ground image processing system (ground segment) as well as for overall performance of the system.

The main body of the flight segment as shown in Figure 1 consists of NASA's standard MMS and the Landsat Instrument Module (IM). The orientation of the spacecraft in its orbit is such that the long dimension of the spacecraft body (the roll axis) lies in the plane of the orbit; the antenna mast is parallel to the local vertical (yaw axis); and the rotation axis of the solar array panels is parallel to the normal to the orbit plane (pitch axis).

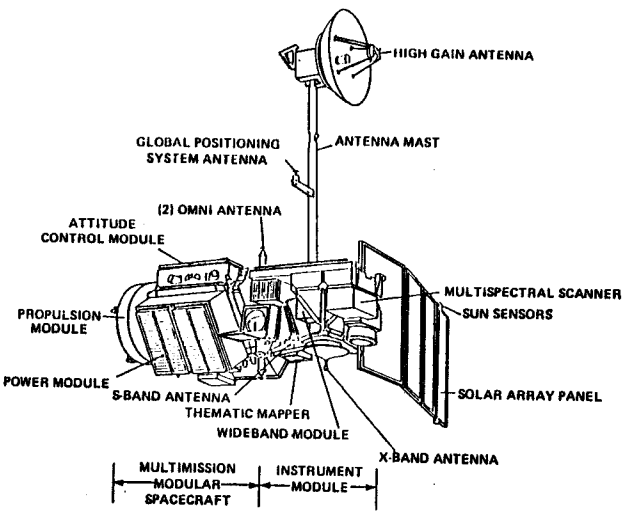

Figure 1. Landsat-D Flight Segment

The IM includes the MSS with optics and scan mechanism compatible with the Landsat-D orbit and the TM instrument of similar design to MSS but with bi-directional scanning. TM has seven spectral bands, six reflective and one thermal.

The Landsat-D Ground Segment consists of a Mission Management Facility which schedules all data acquisition and controls production on the ground; a Control and Simulation Facility which provides flight segment control; and an Image Generation Facility which receives and records image data, radiometrically and geometrically corrects the data and generates archival products.

The ground segment is a highly automated spacecraft control and image processing facility that will provide fast processing. Within the Image Generation Facility, the Thematic Mapper Image Processing System will develop and apply the data needed for geometric interpretation and correction of the imagery. The process of geometric correction data generation is described in the next section.

III GENERATION OF GEOMETRIC CORRECTION DATA

Generation of data for geometric correction of Landsat-D imagery is performed in two steps. The first of these produces systematic correction data, the second geodetic correction data.

Systematic correction data interprets the digital image array in terms of an instrument-spacecraft-rotating earth model. The static parameters of the model are the spacecraft-instrument internal alignments and earth ellipsoid parameters. Dynamic inputs are the measured (or predicted) ephemeris and measured attitude data (0-125 HZ), processed to remove outliers and to provide a time grid of the required resolution. The mirror velocity profile is also determined dynamically.

The major sources of error in systematic correction data are believed to be ephemeris and low frequency attitude data errors. These errors evidence themselves as differences between predicted locations and actual locations of control points or "dislocations" of these ground truth points. The predicted locations are based on measurements in systematically corrected image data.

Geodetic correction of image data is based on the hypothesis that the sources of error in systematic correction data are slowly varying functions of time, and can be expressed as a spacecraft "state error vector". The components of the state error vector are the spacecraft position and attitude errors and their rates, and these are estimated by the recursive distortion estimator.

Thus, the inputs to the computation of geodetic correction data are systematic correction data and control point "dislocations". The essential outputs are estimates of the state error vector components as functions of time. These are used to upgrade systematic correction data to geodetic correction data.

IV THEMATIC MAPPER RECURSIVE DISTORTION ESTIMATOR

The recursive distortion estimator $(RDE)^2$ used for TM geodetic correction consists of three processes - prediction, filtering, and smoothing - that yield an estimate of the state error vector which minimizes the variance of each component.

The equations for the discrete time linear estimation problem are:

$$\delta(t_{k+1}) = \phi(t_{k+1,k})\delta(t_k)+W(t_k), \quad (1)$$

$$Z(t_k) = H(t_k)\delta(t_k)+V(t_k), \quad (2)$$

$$k = 0,1,2,....n,$$

where the variables are defined as follows:

$\delta(t_k)$ - (nx1) state error vector at time t_k - deviation from "true" state vector at t_k

$\phi(t_{k+1,k})$ - (nxn) transition matrix - carries system from t_k to t_{k+1} using dynamic models

$W(t_k)$ - (nx1) vector of system noise at t_k - accumulation of model noise at t_k due to imperfect modeling and calculation

$Z(t_k)$ - (2x1) discrete time measurement vector-CP dislocations in cross track and along track directions

$H(t_k)$ - (2xn) measurement matrix relating the measurement to the state error vector at the position (partial derivatives of the dislocations with respect to components of the state vector)

$V(t_k)$ - (2x1) measurement noise vector associated with $Z(t_k)$

The initial state error vector $\delta(t_o)$ is a Gaussian random variable with $\bar{\delta}(t_o)$ mean and covariance $P(t_o)$.

$W(t_k)$ and $V(t_k)$ are mutually independent zero mean white Gaussian sequences, with covariances given by

$$E\{W(t_k)W^T(t_j)\} = Q(t_k)\Delta_{kj}, \quad (3)$$

$$E\{V(t_k)V^T(t_j)\} = R(t_k)\Delta_{kj}, \quad (4)$$

where:

Q(t) - (nxn) system model noise covariance matrix,
R(t) - (2x2) measurement noise covariance matrix,
Δ - Kronecker delta.

A. PREDICTION

To propagate the dynamic variable $\delta(t_k)$ to a time t_{k+1} (the minus indicates values before the filter update) we need models describing the evolution of $\delta(t)$.

These models are embodied in the transition matrix $\phi(t_{k+1},k)$ which propagates the state vector from the time t_k to t_{k+1}. The equation describing the evolution is

$$\delta(t_{k+1}^-) = \phi(t_{k+1},k)\delta(t_k^+)+W(t_k^+) \quad (5)$$

(where the plus sign indicates values after filter update).

The covariance matrix P(t) obeys a similar propagation equation given by

$$P(t_{k+1}^-) = \phi(t_{k+1,k})P(t_k^+)\phi^T(t_{k+1,k})+Q(t_k) \quad (6)$$

The calculation of the transition matrix for ephemeris is based on the vector equation

$$\frac{d^2\vec{r}}{dt^2} + \frac{\mu}{r^3}\vec{r} = \vec{a} \quad (7)$$

where $\vec{r}$ is the vector position and $\vec{a}$ is a vector of acceleration arising from the presence of the disturbing forces, and is modeled as a white noise process. Let $\vec{r}_o(t)$ be the spacecraft position in an undisturbed (reference) orbit and $\vec{r}(t)$ be the true position vector. The dynamic equations for the state vector $(\vec{r}-\vec{r}_o, \dot{\vec{r}}-\dot{\vec{r}}_o)$ can be obtained by linearization of Equation (7). The form of these equations and, further, the form of the transition matrix depends upon the choice of reference orbit.

The transition matrix for the attitude is based on the following simplified dynamic equations for the gyro angles roll (x_1), pitch (x_2), and yaw (x_3) and their rates (x_4, x_5, and x_6):[3]

$$\begin{aligned} \dot{x}_1 &= \omega x_3 - x_4 + \xi_1; & \dot{x}_4 &= \xi_4; \\ \dot{x}_2 &= -x_5 + \xi_2; & \dot{x}_5 &= \xi_5; \\ \dot{x}_3 &= -\omega x_1 - x_6 + \xi_3; & \dot{x}_6 &= \xi_6. \end{aligned} \quad (8)$$

where ω is the spacecraft orbital rate and ξ_1, ξ_2 and ξ_3 are white Gaussian noise with variance σ_1^2 and ξ_4, ξ_5, and ξ_6 are white Gaussian noise with variance σ_2^2.

The transition matrix for Thematic Mapper dynamic alignment is based on the stochastic process equations[3]

$$\dot{\xi}+\frac{1}{T}\xi = U(t), \quad \text{and} \quad \dot{\eta} = \xi. \quad (9)$$

Here η is the alignment angle and ξ the corresponding rate. U(t) is a white noise process, and T is a time constant. These equations reflect the fact that during the interval of interest the alignment angles may be approximated by integrals of colored noise.

B. FILTERING

This step involves updating $\delta(t_k^-)$ and $P(t_k^-)$ based on the measured control point dislocation at time t_k. Two quantities must be computed before the update can be performed. One is the residual of the measurements $\tilde{Z}(t_k^-)$ given by

$$\tilde{Z}(t_k^-) = Z(t_k) - H(t_k)\delta(t_k^-). \quad (10)$$

$Z(t_k)$ is the measured dislocation and $H(t_k)$ is a measurement matrix whose elements are the partial derivatives of the along track and cross track dislocation with respect to the δ's, so that $H(t_k)\delta(t_k^-)$ is a predicted dislocation.

The other equation defines the Kalman gain matrix $K(t_k)$ as follows:

$$K(t_k) = P(t_k^-)H^T(t_k)\{H(t_k)P(t_k^-)H^T(t_k)+R\}^{-1} \quad (11)$$

These quantities appear in the filter update equations which are:

$$\delta(t_k^+) = \delta(t_k^-)+K(t_k)\tilde{Z}(t_k^-) \quad (12)$$

and

$$P(t_k^+) = P(t_k^-)-K(t_k)H(t_k)P(t_k^-) \quad (13)$$

The difference between the measured and predicted dislocations is used to update $\delta(t_k^-)$ but it is weighted by the Kalman gain matrix, which is a function of the covariance matrix and the measurement noise matrix. If the model errors are dominant then the residual will have a large impact on the update, while a large measurement noise will reduce its effect.

C. SMOOTHING

This step starts with the filtered data and works backward to recursively compute a smoothed estimate of the state error vector. Assuming there are a total of N observations (control point dislocation measurements) for the imagery interval, the last state vector estimate is $\delta(t_N)$ and the last covariance matrix in the filter is $P(t_N)$. Starting with these values the smoother computes a state error vector estimate at the next to last point.

It then uses the smoothed estimate there and filter prediction at the previous point to produce a new smoothed estimate, and so on. The basic equations are[4]

$$C_K=P(t_k^+)\phi^T(t_{k+1,K})P^{-1}(t_{K+1}^-), \quad (14)$$

$$\delta^S(t_k)=\delta(t_k^+)+C_k\{\delta^S(t_{K+1})-\delta(t_{K+1}^-)\}, \quad (15)$$

$$P^S(t_k)=P(t_k^+)+C_K\{P^S(t_{K+1})-P(t_{K+1}^-)\}C_K^T. \quad (16)$$

In Equations 14-16 the index k takes on values from N-1 to 0. The smoothed state error vector estimates are $\delta^S(t_k)$ and the covariance matrix is $P^S(t_k)$.

Smoothing using filtered data is the optimal combination of two estimates, one obtained from a forward filter sweep of the measurements and the other from a backward sweep of the filtered estimates. The smoothing solution presented here is in a recursive form and is used to process the filtered estimates in reverse order, from last to first.

V SIMULATION

In order to test the performance of the recursive distortion estimator, simulation studies[5] were carried out using the ephemeris, attitude, and alignment models described in section IV. The initial values for the model variables were selected randomly based on a priori estimates of the variances of the state error vector elements. These initial elements were then propagated over the interval of interest to determine the state error vector on a grid of evaluation points. The ground dislocations associated with these state error vectors were stored as "real world" data against which the RDE performance could be measured. To produce simulated control point measurements, a given number of control points were randomly selected. Dislocations were computed for these selected control points and corrupted by the addition of a random measurement error (image noise) chosen from Gaussian distributions with cross track variance σ_x^2 and along track variance σ_y^2.

The simulation studies were performed for filter state error vectors of dimension 18 and 12. The 18 variables are ephemeris, alignment, and attitude position and rate errors, while the 12 variables are only ephemeris and alignment errors, that is; the attitude errors are included in the alignment errors.

To produce "real world" data the simulator always used 18 variables. The RDE used both 18 and 12 variables in its models. The effects of attitude and alignment errors on the ground are different, but for time intervals between control points used in this simulation the results involving 12 and 18 variable state error vectors were comparable.

The control point measurements were the inputs which the RDE used to estimate the state error vector at the control points. The estimated state error vectors at the evaluation points were found by interpolation. The estimated state error vectors were multiplied by the measurement matrix to yield estimated control point dislocations. These were compared with the "real world" data described before. The residuals or differences between the estimated and "real world" dislocations were computed at all evaluation points.

The performance of the RDE is typically characterized by the 90 percent residual, ε^{90}, defined as the residual value greater than 90 percent of the residuals in a interval of imagery. This performance measure of the RDE portion of the geometric correction is compared against the system requirement that the RDE residuals be less than 4.9 meters, 90 percent of the time, for a measurement error of 6.7 meters.

ε^{90} is a function of the control point density and the measurement error. Figure 2 illustrates some typical results. Each curve is labeled according to the density of control points (control points per scene) and the number of variables used in the RDE (18 or 12). Approximately 100 realizations were run to obtain a statistically significant value for each point. As expected, the ε^{90} residual value improves as the control point density increases and the measurement error decreases. The 18 and 12 variable cases give comparable results.

The density of control points needed to meet the system requirements stated above is plotted as a function of imagery interval length in Figure 3. The density required for intervals greater than 10 scenes is stable at about 3 control points per scene.

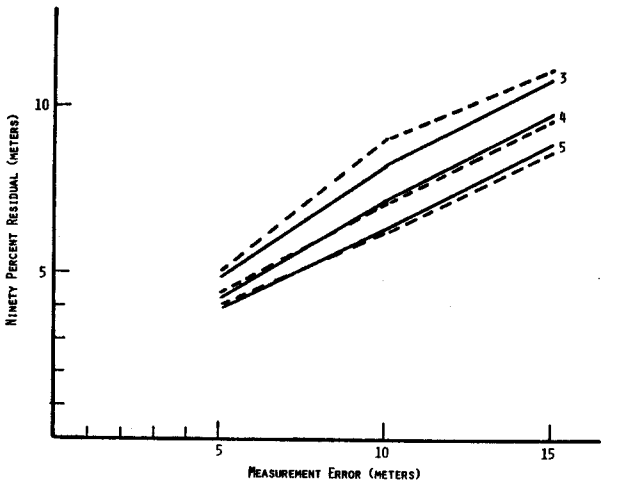

Figure 2. Ninety Percent Residual as a Function of Measurement Error. Solid lines are for the 18 variable state error vectors, and dashed lines are for the 12 variable state error vectors. Numbers next to curves are control point densities. Results are shown for a five scene interval.

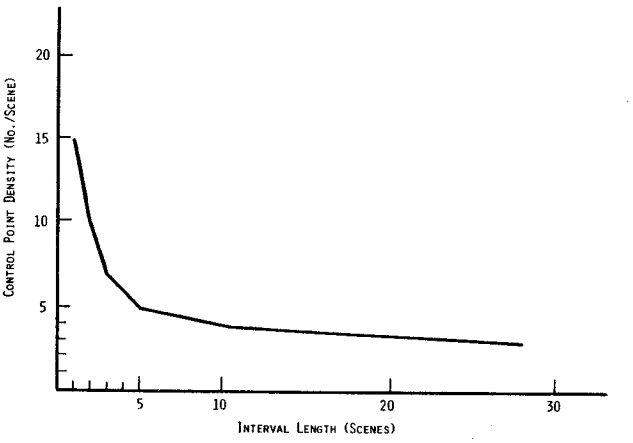

Figure 3. Control Point Density Needed to Meet System Requirements as a Function of Interval Length.

VI SUMMARY

The RDE was successfully adapted for use in the Thematic Mapper geodetic correction data generation. This method offers advantages in the case of interval processing because it minimizes the number of control points needed per scene, it provides continuity of correction across scene boundaries, and provides for correction of embedded scenes with few or no control points.

ACKNOWLEDGMENTS

This work was supported by NASA under contract no. NAS5-25300. We acknowledge the work of the Mission Systems Engineering Group (General Electric Space Systems Division) in developing some of the models used in the RDE.

REFERENCES

1. J. Brooks, I. Levine, D. Poros, "A Conceptual Design of the Geodetic Error Determinator for TM Imagery," General Electric Co., Space Division, 1T81-LSD-SYS.ANALYSIS-MEMO-17, 1981.
2. P.S. Maybeck, "Stochastic Models, Estimator, and Control," Volume 1, Academic Press, 1979.
3. T.F. Green, "A Summary of Measurement Processing Models," General Electric Co., Space Systems Division, PIR No.1K50-LSD-334, 1979.
4. H.E. Rauch, "Linear Smoothing Techniques," in "Theory and Applications of Kalman Filtering," AGARDograph No.139, Edited by C.T. Leondes, 1970.
5. E. Kimmer, V. Matthews, "Simulation Studies of the GED," General Electric Co., Space Systems Division, PIR No. 1T81-LSD-GS-363, 1981.

Paul E. Arnold received his B.S. in Mathematics from Howard University in 1972. He received his M.A. in Mathematics from the University of Maryland in 1974. He joined G.E. in 1979 as a Systems Analyst and has worked on the design and analysis of the Landsat-D image processing system.

Joan Brooks completed here B.A. and Ph.D. degrees in Physics at New York University and has divided her professional life between university and industry. Her fields of specialization are physical optics, particle transport theory and, more recently, satellite image processing techniques.

Edward Kimmer received his Ph.D. degree in Astrophysics from the University of Toledo in 1976. Since then he has been involved with processing and analysis of data from Earth satellites. He is currently a Systems Analyst in the General Electric Space Division, working on the Landsat-D image processing system.

Igor Levine, Ground Systems Analyst, joined General Electric in 1979 and has worked on the design and analysis of Landsat-D image processing system. He has developed a perturbation technique of geometric correction of Landsat-type imagery, developed the MSS Control Point Location Error Filter and carried out its simulation studies. He holds a M.S. degree in Electrical Engineering from Leningrad Polytechnic Institute, a M.S. degree in Mathematics from Leningrad University, and a Ph.D. degree in Computer Science from Radio Electronics Research Institute (Leningrad, U.S.S.R.).

Valerie H. Matthews received the B.S. degree in mathematics from the University of Maryland, College Park, Maryland, in 1981. She is currently working on simulation software and operational software for the Landsat-D image processing system.

Demetrios J. Poros received his B.S. in mathematics from University of Athens, Greece, his M.A. in mathematics from Boston University and continued studies in applied mathematics at the University of Maryland. He joined General Electric in 1979 and has been active in algorithm development for the Landsat-D image processing system. His current interest is in application of Kalman filtering and Partial Differential Equations to recursive image restoration.